In Vivo Insulin Resistance Induced by Amylin Primarily Through Inhibition of Insulin-Stimulated Glycogen Synthesis in Skeletal Muscle

SIMONA FRONTONI, SOO BONG CHOI, DONNA BANDUCH, AND LUCIANO ROSSETTI

We examined the in vivo mechanisms of amylin-induced resistance in concious rats (n = 18). During 180-min euglycemic insulin-clamp (21.5 pmol · kg^{-1} · min^{-1}) studies, amylin (50, 200, or 500 pmol · kg^{-1} · min^{-1}; plasma concentration from 3 × 10^{-10} to 9 × 10^{-9} M) infusion determined a 19–27% reduction in glucose uptake (117.8 ± 7.0 vs. 145.8 ± 11.0, 107.1 ± 9.2 vs. 145.1 ± 6.7, and 105.0 ± 7.2 vs. 144.4 ± 7.0 μmol · kg^{-1} · min^{-1} at 50, 200, or 500 pmol · kg^{-1} · min^{-1}, respectively, $P < 0.01$) versus insulin alone, whereas 10-pmol · kg^{-1} · min^{-1} amylin infusion (plasma concn 5 × 10^{-11} M) failed to affect insulin-mediated glucose disposal. After amylin infusion, the contribution of whole-body glycolysis to overall glucose disposal increased from 43–48 to 62–79%, whereas muscle glycogen synthesis decreased significantly at all peptide concentrations >3 × 10^{-10} M, completely accounting for the decrease in glucose uptake. Skeletal muscle glucose-6-phosphate concentration rose from 0.219 ± 0.038 μmol/g (insulin alone) to 0.350 ± 0.018, 0.440 ± 0.020, and 0.505 ± 0.035 μmol/g (insulin plus amylin at 50, 200, or 500 pmol · kg^{-1} · min^{-1}, $P < 0.01$). Suppression of hepatic glucose production by insulin was unaffected by a 50-pmol · kg^{-1} · min^{-1} amylin infusion (18.5 ± 4.3 vs. 21.7 ± 2.9 μmol · kg^{-1} · min^{-1}), whereas it was slightly but significantly impaired by amylin infusion at 200 pmol · kg^{-1} · min^{-1} (17.8 ± 3.9 vs. 24.7 ± 4.5 μmol · kg^{-1} · min^{-1}, $P < 0.05$). At higher plasma concentrations (8.7 × 10^{-9} M), amylin further stimulated hepatic glucose production (52.2 ± 3.3 μmol · kg^{-1} · min^{-1}, $P < 0.05$), whereas peripheral glucose uptake and muscle glycogen synthesis were not further reduced. Our results suggest that amylin antagonizes the ability of insulin to promote total-body glucose uptake primarily by decreasing muscle glycogen synthesis, which, in turn, determines an increase in muscle glucose-6-phosphate levels and glycolysis and a reduction in glucose transport/phosphorylation. *Diabetes* 40:568–73, 1991

Since the original observation by Opie (1,2) of hyaline infiltration in islets of a diabetic subject, interstitial deposits of amyloid have been documented in 77–87% of the pancreatic islets from non-insulin-dependent (type II) diabetic individuals (3–7). These interstitial amyloid deposits are relatively specific for type II diabetes (1–4) and, in spontaneously diabetic monkeys, precede the onset of glucose intolerance (8,9). The major protein constituent of pancreatic amyloid has been identified in a 37–amino acid peptide (known as *islet amyloid polypeptide, IAPP,* or *amylin*), which has been sequenced after isolation from amyloid of pancreatic islets of type II diabetic subjects (10,11) and displays a 46% homology with calcitonin gene–related peptide (CGRP), an alternative splice product of the calcitonin gene (10,12). Amylin and insulin have been demonstrated to be colocalized within β-cell secretory granules and to be coreleased in a molar ratio after stimulation by glucose and nonglucose secretagogues both in rats (13) and humans (14,15). Although CGRP has been shown to inhibit insulin secretion in isolated pancreatic islets (16), amylin failed to regulate insulin biosynthesis or secretion in normal rat islets (17). Purified amylin extracted from diabetic pancreases, synthetic amylin, and CGRP have also been assessed for their ability to inhibit insulin action in vitro (11,18) and in vivo (19,20). In particular, recent studies have demonstrated that both amylin and CGRP are potent inhibitors of glycogen synthesis in isolated soleus muscle (18). Although Ghatei et al. (21) and Bretherton-Watt et al. (22) failed to demonstrate an acute effect of amylin on blood glucose and insulin concentration in rabbits and humans, Molina et al. (20) and Sowa et al. (19) in anesthetized rats and dogs, respectively, showed the induction of insulin resistance by amylin infusion with the euglycemic clamp

From the Department of Medicine, University of Texas Health Science Center, San Antonio, Texas.

Address correspondence and reprint requests to Luciano Rossetti, MD, Diabetes Division, Department of Medicine, University of Texas Health Science Center, 7703 Floyd Curl Drive, San Antonio, TX 78284-7886.

Received for publication 17 August 1990 and accepted in revised form 26 December 1990.

technique. These findings have prompted speculation concerning the role of amylin in the pathophysiology of type II diabetes (23). However, the observation by Butler et al. (15) of similar basal and postmeal plasma amylin concentrations in type II subjects compared with control subjects seems to deny a role for the peptide in the pathophysiology of insulin resistance in type II diabetes, although the possibility that amylin concentration may be increased in an earlier stage in the natural history of diabetes mellitus remains to be investigated. Observations in siblings of type II diabetic subjects (24) and in spontaneously diabetic monkeys (9) suggest that a reduced ability of insulin to stimulate nonoxidative glucose disposal (mainly glycogen synthesis) is an early characteristic of the diabetic state. Thus, it is important to delineate the metabolic characteristics of amylin-induced insulin resistance at different plasma amylin concentrations.

The aim of this study was to investigate the acute effects of amylin on glucose metabolism in conscious rats and to delineate the metabolic pathways and tissues involved in its effects.

RESEARCH DESIGN AND METHODS

Male Sprague-Dawley rats (250–300 g; Harlan, Indianapolis, IN) were studied. The rats were given free access to food and water, housed in individual cages in an air-controlled room, and subjected to a standard light- (0600–1800) dark (1800–0600) cycle.

Five to 7 days before the experiment, all animals were anesthetized with pentobarbital sodium (50 mg/kg i.p. body wt), and indwelling catheters were inserted in the right internal jugular vein and in the left carotid artery. The venous catheter was extended to the level of the right atrium, and the arterial catheter was advanced to the level of the aortic arch. Both catheters were exteriorized through the skin at the back of the neck.

Euglycemic insulin/amylin infusions. Whole-body glucose uptake and hepatic glucose production were measured in awake, unrestrained, chronically catheterized rats with the euglycemic clamp in combination with [3-^{3}H]glucose infusion as previously described (25–27) (Fig. 1). Briefly, at 0900 after a 24-h fast, rats received an infusion of 21.5 pmol · kg^{-1} · min^{-1} insulin for 3 h, and during the last 90 min of the study, an infusion of amidated human amylin (10, 50, 200, or 500 pmol · kg^{-1} · min^{-1}; Sigma, St. Louis, MO) was superimposed. Amylin stock solution was prepared in distilled water plus 0.5% bovine serum albumin and then adjusted with acetic acid to a pH between 5 and 6.5. The solution was diluted to the desired concentration with normal saline. In all studies, a variable infusion of 25% glucose solution was started at time 0 and adjusted to clamp the plasma glucose concentration at ~5.6 mM. A primed (2-μCi) continuous (0.4-μCi/min) infusion of [3-^{3}H]glucose (Du Pont-NEN, Boston, MA) was initiated at time 0 and continued throughout the study (25–27). A primed (1-μCi) continuous (0.2-μCi/min) infusion of [U-^{14}C]glucose (Du Pont-NEN) was initiated at 90 min and continued throughout the study. Plasma samples for determination of [3-^{3}H]- and [U-^{14}C]glucose specific activities were obtained at 5- to 10-min intervals throughout the studies. The [U-^{14}C]glucose infusion was used to quantitate the rate of net glycogen synthesis during the amylin infusion period (last 90 min of the insulin-clamp study). Plasma samples for determination of plasma insulin and amylin concentrations were obtained at −30, 0, 60, 90, 150, and 180 min during the study.

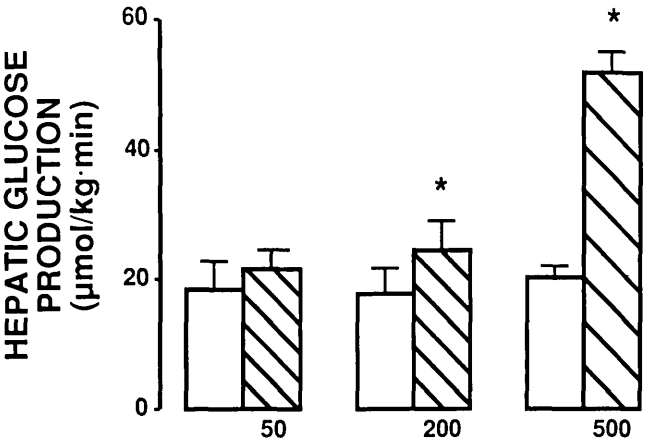

FIG. 1. Hepatic glucose production. Rats received infusion of 21.5 pmol · kg^{-1} · min^{-1} insulin for 3 h (*open bars*) and, during last 90 min of study, infusion of 50, 200, or 500 pmol · kg^{-1} · min^{-1} amidated human amylin was superimposed (*hatched bars*). In all studies, variable infusion of 25% glucose solution was started at time 0 and adjusted to clamp plasma glucose concentration at ~5.6 mM. A primed (2-μCi) continuous (0.4-μCi/min) infusion of [3-^{3}H]glucose was initiated at time 0 and continued throughout study. Primed (1-μCi) continuous (0.2-μCi/min) infusion of [U-^{14}C]glucose was initiated at 90 min and continued throughout study. Basal hepatic glucose production, measured during separate saline infusion studies, was 38.6 ± 0.7 μmol · kg^{-1} · min^{-1}.

The total amount of blood withdrawn during each study was ~2.5 ml. To prevent intravascular volume depletion and anemia, an equivalent amount of normal saline (1 ml) plus fresh whole blood (1.5 ml blood) obtained by heart puncture from littermates of the test animal was infused at a constant rate (14 μl/min) throughout the study. At the end of the study, rats were injected with pentobarbital sodium (60 mg/kg body wt), the abdomen was quickly opened, and the rectus abdominal and hindlimb muscles were freeze-clamped with aluminum tongs precooled in liquid N_2. All tissue samples were kept frozen at −80°C for subsequent analysis. The study protocol was reviewed and approved by the Institutional Animal Care and Use Committee of the University of Texas Health Science Center at San Antonio.

Glycogen formation in vivo. Muscle glycogen synthesis during insulin infusion was quantitated by measuring both the incorporation of [3-^{3}H]glucose and [U-^{14}C]glucose counts into glycogen and the increment in glycogen concentration from basal levels. Muscle glycogen concentration was determined after digestion with glucan 1,4-α-glucosidase as previously described (26,27). The intra-assay and interassay coefficients of variation for muscle glycogen were <10%. Alliquots of the tissue homogenate (200 μl) were used to determine the amount of ^{3}H and ^{14}C label in glycogen. Glycogen was precipitated by washing in 10 vol absolute ethanol and incubating for 1 h at −20°C. The procedure was repeated three times, then the precipitate was collected, dried down, and dissolved in water before scintillation counting. The recovery of free [3-^{3}H]glucose, added to test the procedure, was <1% of the free glucose radioactivity added to the homogenate in each assay.

Whole-body glycolytic rate. Aliquots of plasma were precipitated with $Ba(OH)_2$ and $ZnSO_4$ and centrifuged. Plasma ^3H_2O specific activity was determined by liquid-scintillation counting of the protein-free supernatant (Somogyi filtrate) before and after evaporation to dryness. ^3H in the C-3 position of glucose is lost selectively to water during glycolysis. Therefore, plasma tritiated counts can be present either as ^3H_2O or [3-^{3}H]glucose (28). Therefore, the difference in tritiated counts before and after evaporation can be assumed to represent the concentration of ^3H in plasma water. Rates of whole-body glycolysis were estimated from the increment per unit time in ^3H_2O (dpm · L^{-1} · min^{-1}) times body water mass (L) divided by the [3-^{3}H]glucose specific activity (dpm/μmol). Plasma water is assumed to be 93% of the total plasma volume, and total body water mass is assumed to be 65% of the body mass (29).

Analytical procedures. Plasma glucose was measured by the glucose oxidase method (glucose analyzer, Beckman, Palo Alto, CA) and plasma insulin by radioimmunoassay with rat and pork insulin standards. After elution through a Sep-Pak C-18 cartridge (Waters), plasma amylin was measured by radioimmunoassay with a kit according to the manufacturer's specifications (Peninsula, Belmont, CA). Plasma [3-^{3}H]glucose radioactivity was measured in duplicate on the supernatants of $Ba(OH)_2$–$ZnSO_4$ precipitates (Somogyi procedure) of plasma samples after evaporation to dryness to eliminate ^3H_2O. Plasma [U-^{14}C]glucose radioactivity was measured in duplicate after purification by ion-exchange chromatography, as previously described (30).

Glucose-6-phosphate (G6P) concentration was measured in freeze-clamped in situ rectus abdominal muscle by enzymatic assay (31).

Calculations. Data for total-body glucose uptake and suppression of hepatic glucose production represent the mean values during the last 30 min of each 90-min period of the insulin-clamp study. The hepatic glucose production was calculated as the difference between the tracer-derived rate of appearance and the infusion rate of cold glucose. Total-body glucose disposal was calculated by adding the rate of residual hepatic glucose production during the last 30 min of each insulin-clamp study to the mean glucose infusion rate during the same 30-min period. The rate of net glycogen synthesis was calculated as the [3-^{3}H]glucose or [U-^{14}C]glucose radioactivity in glycogen (dpm/kg tissue) divided by the time-weighted mean specific activity of [3-^{3}H]- or [U-^{14}C]glucose in plasma during the insulin clamp (dpm/μmol plasma glucose). The rate of net glycogen synthesis is expressed as micromoles of glucose in glycogen per kilogram of tissue (26,27). The rate calculated from the [^{14}C]glucose incorporation into glycogen measured muscle glycogen synthesis during the amylin/insulin infusion period. The rates of net glycogen synthesis during the infusion of insulin alone (first 90 min of insulin-clamp study) were obtained by subtracting the muscle glycogen synthesized during the amylin infusion from the total amount of muscle glycogen synthesized during the insulin-clamp study. For each rat, the means of four determinations on rectus abdominal muscle and four on hindlimb muscle were used to approximate the mean whole-body muscle glycogen concentration. All values are presented as means ± SE. Differences between groups were determined with paired or unpaired Student's *t* test, as appropriate.

TABLE 1
Mean ± SE steady-state plasma glucose (SSPG), steady-state plasma insulin (SSPI), and plasma amylin concentrations during euglycemic-hyperinsulinemic clamp studies

	SSPG (mM)	SSPI (pM)	Amylin (pM)
Control	5.8 ± 0.2	249 ± 18	
+10 pmol amylin	5.7 ± 0.3	222 ± 27	51 ± 11
Control	5.6 ± 0.2	251 ± 27	
+50 pmol amylin	5.7 ± 0.1	261 ± 19	328 ± 39
Control	5.8 ± 0.2	245 ± 36	
+200 pmol amylin	5.7 ± 0.1	222 ± 37	1610 ± 137
Control	5.6 ± 0.2	241 ± 26	
+500 pmol amylin	5.8 ± 0.1	269 ± 32	8709 ± 412

Amylin was infused at 50, 200, or 500 pmol · kg^{-1} · min^{-1} during last 90 min of insulin-clamp study.

RESULTS

Steady-state plasma glucose and insulin concentrations during the insulin-clamp studies were similar with or without amylin infusion (Table 1). The coefficients of variation in plasma glucose and insulin levels were <5% and <10%, respectively, in all studies. The steady-state plasma amylin concentrations during the infusion are shown in Table 1. From basal concentrations of <20 pM, amylin rose to 51 ± 11, 328 ± 39, 1610 ± 137, and 8709 ± 412 pM during the 10-, 50-, 200-, and 500-pmol · kg^{-1} · min^{-1} infusion rates, respectively. Amylin infusion at 10 pmol · kg^{-1} · min^{-1} did not affect any parameter of insulin-mediated glucose metabolism. During hyperinsulinemia, hepatic glucose production was suppressed by 50% in all control studies. The hepatic glucose production was unchanged (18.5 ± 4.3 vs. 21.7 ± 2.9 μmol · kg^{-1} · min^{-1}) during the 50-pmol · kg^{-1} · min^{-1} amylin infusion but was slightly, although significantly, increased after the 200-pmol · kg^{-1} · min^{-1} amylin administration (24.7 ± 4.5 vs. 17.8 ± 3.9 μmol · kg^{-1} · min^{-1}, $P < 0.05$). However, when amylin concentration rose further to ~10^{-8} M, hepatic glucose production was significantly stimulated from 20.5 ± 1.7 to 52.2 ± 3.3 μmol · kg^{-1} · min^{-1}

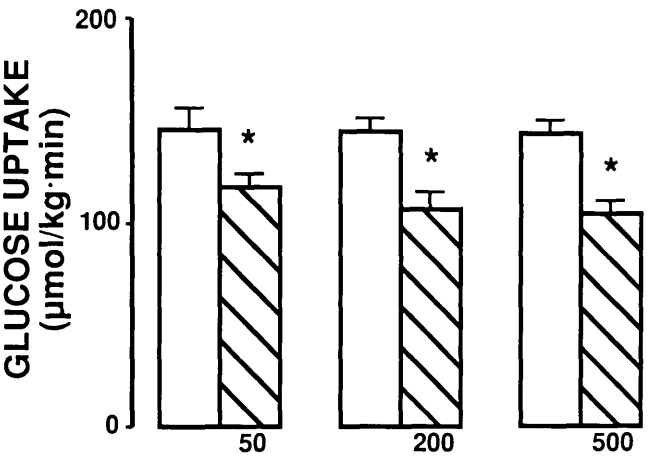

FIG. 2. Glucose uptake during infusion of insulin alone (*open bars*) and insulin plus amylin (*hatched bars*) in control rats. One hundred eighty–minute euglycemic clamp studies were performed with physiological insulin concentrations (~250 pmol/ml), and 50, 200, and 500 pmol · kg^{-1} · min^{-1} amylin was superimposed during last 90 min. *Bars*, means ± SE of last 30 min of each period (60–90 and 150–180 min). *$P < 0.001$ vs. insulin alone.

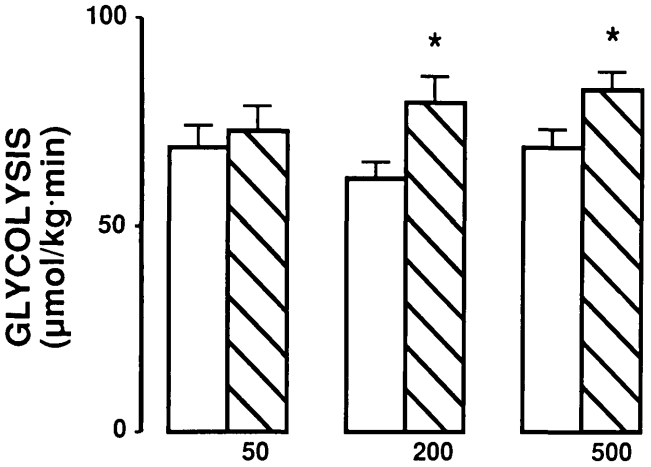

FIG. 3. Glycolysis during infusion of insulin alone (*open bars*) and insulin plus amylin (*hatched bars*) in control rats. One hundred eighty–minute euglycemic clamp studies were performed with physiological insulin concentrations (~250 pmol/ml), and 50, 200, and 500 pmol · kg^{-1} · min^{-1} amylin was superimposed during last 90 min. *Bars*, means ± SE of last 30 min of each period (60–90 and 150–180 min). *$P < 0.05$ vs. insulin alone.

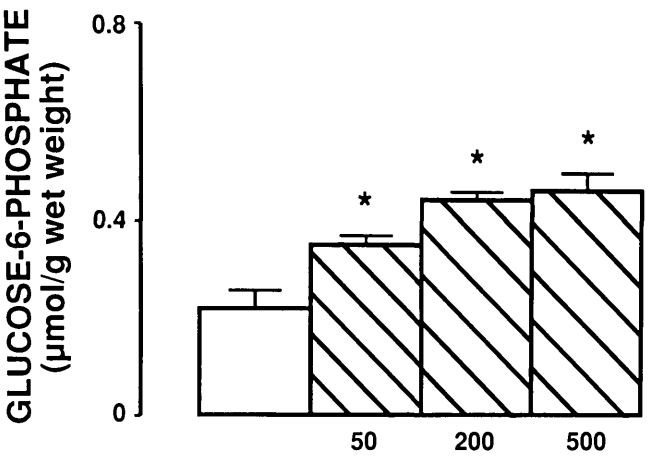

FIG. 5. Skeletal muscle glucose-6-phosphate concentration at end of euglycemic insulin-clamp studies without (*open bar*) and with (*hatched bars*) 50, 200, and 500 pmol · kg^{-1} · min^{-1} amylin. Muscle glucose-6-phosphate was significantly increased with amylin infusion. *$P < 0.01$.

(Fig. 1). Therefore, amylin antagonizes the insulin action on hepatic glucose production only at high plasma concentration of the peptide.

By contrast, the insulin-mediated whole-body glucose uptake (~145 μmol · kg^{-1} · min^{-1}) decreased significantly during 50- (117.8 ± 7.0 μmol · kg^{-1} · min^{-1}, $P < 0.01$), 200- (107.1 ± 9.2 μmol · kg^{-1} · min^{-1}, $P < 0.01$), and 500- (105.0 ± 7.2 μmol · kg^{-1} · min^{-1}; $P < 0.01$) pmol · kg^{-1} · min^{-1} amylin infusions (Fig. 2). During the amylin infusions, the contribution of whole-body glycolysis to total glucose disposal increased from 43–49% to 62–75% (Fig. 3), whereas the contribution of muscle glycogen synthesis (Fig. 4) was markedly reduced (35.6 ± 3.2 vs. 69.6 ± 5.2, 17.7 ± 2.4 vs. 77.7 ± 7.7, and 14.3 ± 3.6 vs. 69.8 ± 4.2 μmol · kg^{-1} · min^{-1} at 50, 200, and 500 pmol · kg^{-1} · min^{-1} amylin, respectively; $P < 0.01$). The defect in muscle glycogen synthesis completely accounted for the reduction observed in overall glucose disposal after all three amylin infusion rates.

Skeletal muscle G6P concentration was significantly increased after amylin infusion (0.219 ± 0.038 vs. 0.350 ± 0.018, 0.440 ± 0.020, and 0.505 ± 0.035 μmol/g wet wt at 50, 200, and 500 pmol · kg^{-1} · min^{-1}, respectively, $P < 0.01$) compared with the concentration measured at the end of euglycemic (21.5 pmol · kg^{-1} · min^{-1}) insulin-clamp studies (Fig. 5).

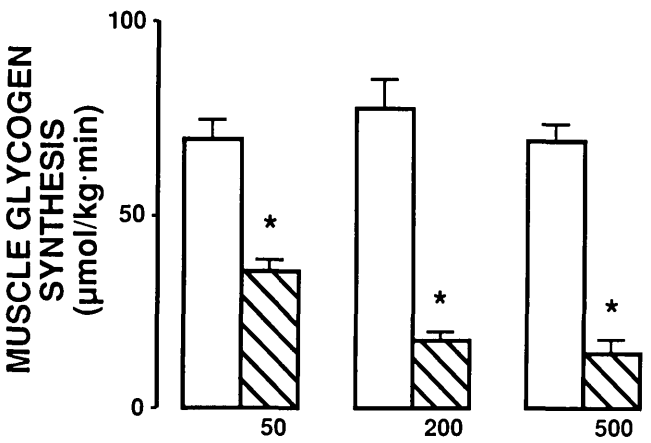

FIG. 4. Muscle glycogen synthesis during infusion of insulin alone (*open bars*) and insulin plus amylin (*hatched bars*) in control rats. One hundred eighty–minute euglycemic clamp studies were performed with physiological insulin concentrations (~250 pmol/ml) and 50, 200, and 500 pmol · kg^{-1} · min^{-1} amylin was superimposed during last 90 min. *Bars*, means ± SE of last 30 min of each time period (60–90 and 150–180 min). *$P < 0.01$ vs. insulin alone.

DISCUSSION

This study defines the acute metabolic effects of amylin on glucose metabolism in conscious rats and delineates the metabolic pathways primarily involved in its effect. Our results demonstrate that the primary site of in vivo action of amylin on insulin-mediated glucose metabolism is the inhibition of glycogen deposition in skeletal muscle. The impairment of insulin's ability to stimulate nonoxidative glucose disposal (glycogen synthesis in skeletal muscle) represents a major characteristic of insulin-resistant type II diabetic individuals (32–34). Data suggest that this alteration may be a major determinant in the pathophysiology of type II diabetes because it appears to precede the onset of glucose intolerance (24).

Because recent studies have determined that the circulating amylin concentration is ~10^{-11} M in humans (13–15), to address the possible role of amylin in the pathophysiology of insulin resistance, it appears important to evaluate both the dose-response relationship between the plasma amylin concentration and insulin sensitivity in conscious animals and the metabolic pathways involved in the metabolic effects of the peptide as a function of its plasma concentration.

In this study, the infusion of 10 pmol · kg^{-1} · min^{-1} amylin (plasma concn 5 × 10^{-11} M) did not affect insulin-mediated glucose metabolism, whereas the infusion of 500 pmol · kg^{-1} · min^{-1} amylin (plasma concn ~10^{-8} M) during euglycemic clamp studies determined the onset of severe insulin resistance through a 32% reduction in insulin-mediated glucose uptake and a 2.5-fold increase in hepatic glucose production. At these pharmacological amylin concentrations, both reduction in glucose uptake (60%) and stimulation of hepatic glucose production (40%) contributed to the overall

impairment in insulin-mediated glucose metabolism. These findings confirm and extend previous observations in anesthetized dogs (19) and rats (20). However, when the effect of amylin on in vivo insulin action was examined at lower concentrations (3×10^{-10} and 1.6×10^{-9} M), the impairment in insulin-mediated glucose metabolism was almost entirely accounted for by a 19–26% reduction in peripheral glucose uptake, whereas the ability of insulin to suppress hepatic glucose production was only marginally affected. Thus, skeletal muscle appears to be more sensitive than liver to the in vivo action of amylin, and the circulating amylin concentration determines the metabolic pathways and tissues involved in its effect on insulin-stimulated glucose metabolism.

Our data may also help elucidate the intracellular mechanism by which amylin causes insulin resistance in vivo. In fact, after amylin administration, we observed a 77% reduction in insulin-stimulated muscle glycogen synthesis. This is in agreement with data in vitro showing that amylin, in concentrations similar to those reached in the plasma during this study (10^{-9} M), significantly decreases the rates of glycogen synthesis in isolated soleus muscle (18). In contrast, we detected a slight but significant increase in insulin-stimulated whole-body glycolysis. The concentration of G6P in skeletal muscle may help further elucidate these findings. In fact, once glucose enters the cell, it is first converted to G6P and then metabolized in the glycolytic or in the glycogen synthetic pathway. Our data show that muscle G6P concentration was significantly increased after amylin infusion. This, taken together with the decreased flux through glycogen synthesis and the increased flux through glycolysis, suggests that amylin primarily inhibits muscle glycogen synthesis, thus determining a rise in G6P concentration, which in turn enhances glycolytic flux and inhibits glucose transport and/or phosphorylation.

Several studies have identified specific receptors for CGRP linked to adenylate cyclase activation (35). Morishita et al. (36) have provided evidence that amidated amylin (10^{-7}–10^{-8} M) interacts with the CGRP receptor present on rat liver plasma membranes to activate adenylate cyclase. Although the plasma amylin concentration acutely affecting glucose metabolism is higher than that commonly observed in humans (13–15) and animals (19), our experiments do not rule out the possibility that amylin levels in the bloodstream may be temporarily elevated in an early phase of the diabetic state and may act in concert with CGRP on the CGRP-effector system in antagonizing insulin action on skeletal muscle glycogen synthesis.

ACKNOWLEDGMENTS

We thank Stella Merla for expert secretarial assistance. This work was supported by grants to L.R. from the American Heart Association (900671) and the American Diabetes Association. S.F. is the recipient of a fellowship from the Italian Consiglio Nazionale delle Ricerche.

REFERENCES

1. Opie EL: On the relation of chronic interstitial pancreatitis to the islands of Langerhans and to diabetes mellitus. *J Exp Med* 5:397–428, 1900–1901
2. Opie EL: The relation of diabetes mellitus to lesions of the pancreas: hyaline degeneration of the islets of Langerhans. *J Exp Med* 5:527–40, 1900–1901
3. Maloy AL, Longnecker DS, Greenberg ER: The relation of islet amyloid to the clinical type of diabetes. *Hum Pathol* 12:917–22, 1981
4. Bell ET: Hyalinization of the islets of Langerhans in non-diabetic individuals. *Am J Pathol* 35:801–805, 1959
5. Clark A, Saad MF, Nezzer T, Uren C, Knowler WC, Bennett PH, Turner RC: Islet amyloid polypeptide in diabetic and non-diabetic Pima Indians. *Diabetologia* 33:285–89, 1990
6. Clark A, Wells CA, Buley ID, Cruickshank JK, Vanhegan RI, Matthews DR, Cooper GJS, Holman RR, Turner RC: Islet amyloid, increased A-cells, reduced B-cells and exocrine fibrosis: quantitative changes in the pancreas in type 2 diabetes. *Diabetes Res* 9:151–60, 1988
7. Westermark P, Wilander E, Westermark GT, Johnson KH: Islet amyloid polypeptide-like immunoreactivity in the islet B cells of type 2 (non-insulin-dependent) diabetic and non diabetic individuals. *Diabetologia* 30:887–92, 1987
8. Bodkin NL, Metzger BL, Hansen BC: Hepatic glucose production and insulin sensitivity preceding diabetes in monkeys. *Am J Physiol* 256:E676–81, 1989
9. Howard CF: Longitudinal studies on the development of diabetes in individual macaca nigra. *Diabetologia* 29:301–306, 1986
10. Cooper GJS, Willis AC, Clark A, Turner RC, Sim SB, Reid KBM: Purification and characterization of a peptide from amyloid-rich pancreases of type 2 diabetic patients. *Proc Natl Acad Sci USA* 84:8628–32, 1987
11. Cooper GJS, Leighton B, Dimitriadis GD, Parry-Billings M, Kowalchuk JM, Howland K, Rothbard JB, Willis AC, Reid KBM: Amylin found in amyloid deposits in human type 2 diabetes mellitus may be a hormone that regulates glycogen metabolism in skeletal muscle. *Proc Natl Acad Sci USA* 85:7763–66, 1988
12. Westermark P, Wernstedt C, Wilander E, Hayden DW, O'Brien TD, Johnson KD: Amyloid fibrils in human insulinoma and islets of Langerhans of the diabetic cat are derived from a neuropeptide-like protein also present in normal islet cells. *Proc Natl Acad Sci USA* 84:3881–85, 1987
13. Kahn SE, D'Alessio DA, Schwartz MW, Fujimoto WY, Ensinck JW, Taborsky GJ Jr, Porte D Jr: Evidence of cosecretion of islet amyloid polypeptide and insulin by β-cells. *Diabetes* 39:634–38, 1990
14. Mitsukawa T, Takemura J, Asai J, Nakazato M, Kangawa K, Matsuo H, Matsukura S: Islet amyloid poloypeptide response to glucose, insulin, and somatostatin analogue administration. *Diabetes* 39:639–42, 1990
15. Butler PC, Chou J, Carter WB, Wang Y-N, Bu B-H, Chang D, Chang J-K, Rizza RA: Effects of meal ingestion on plasma amylin concentration in NIDDM and nondiabetic humans. *Diabetes* 39:752–56, 1990
16. Ahre'n B, Martensson H, Nobin A: Effects of calcitonin gene–related peptide (CGRP) on islet hormone secretion in the pig. *Diabetologia* 30:354–59, 1987
17. Nagamatsu S, Carroll RJ, Grodsky GM, Steiner DF: Lack of islet amyloid polypeptide regulation of insulin biosynthesis or secretion in normal rat islets. *Diabetes* 39:871–74, 1990
18. Leighton B, Cooper GJS: Pancreatic amylin and calcitonin gene related peptide causes resistance to insulin in skeletal muscle in vitro. *Nature* (Lond) 335:632–35, 1988
19. Sowa R, Sanke T, Hirayama J, Tabata H, Furuta H, Nishimura S, Nanjo K: Islet amyloid polypeptide amide causes peripheral insulin resistance in vivo in dogs. *Diabetologia* 33:118–20, 1990
20. Molina JM, Cooper GJS, Leighton B, Olefsky JM: Induction of insulin resistance in vivo by amylin and calcitonin gene–related peptide. *Diabetes* 39:260–65, 1990
21. Ghatei MA, Datta HK, Zaidi M, Bretherton-Watt D, Wimalawansa SJ, MacIntyre I, Bloom SR: Amylin and amylin-amide lack an acute effect on blood glucose and insulin. *J Endocrinol* 124:R9–11, 1990
22. Bretherton-Watt D, Gilbey SG, Ghatei MA, Beacham J, Bloom SR: Failure to establish islet amloid polypeptide (amylin) as a circulating beta cell inhibiting hormone in man. *Diabetologia* 33:115–17, 1990
23. Porte D Jr, Kahn SE: Hyperproinsulinemia and amyloid in NIDDM: clues to etiology of islet β-cell dysfunction? *Diabetes* 38:1333–36, 1989
24. Eriksson J, Franssila-Kallunki A, Ekstrand A, Saloranta C, Wide'n E, Schalin C, Groop L: Early metabolic defects in persons at increased risk for non-insulin-dependent diabetes mellitus. *N Engl J Med* 321:337–43, 1989
25. Rossetti L, Smith D, Shulman GI, Papachristou D, DeFronzo RA: Correction of hyperglycemia with phlorizin normalizes tissue sensitivity to insulin in diabetic rats. *J Clin Invest* 79:1510–15, 1987
26. Rossetti L: Normalization of insulin sensitivity with lithium in diabetic rats. *Diabetes* 38:648–52, 1989
27. Rossetti L, Laughlin MR: Correction of chronic hyperglycemia with vanadate, but not phlorizin, normalizes in vivo glycogen repletion and in vitro glycogen synthase activity in diabetic skeletal muscle. *J Clin Invest* 84:892–99, 1989
28. Young AA, Bogardus C, Wolfe-Lopez D, Mott DM: Muscle glycogen synthesis and disposition of infused glucose in humans with reduced rates of insulin-mediated carbohydrate storage. *Diabetes* 37:303–308, 1988
29. Rossetti L, Giaccari A: Relative contribution of glycogen synthesis and glycolysis to insulin-mediated glucose uptake: a dose-response euglycemic clamp study in normal and diabetic rats. *J Clin Invest* 85:1785–92, 1990
30. Shulman GI, Rossetti L, Rothman DL, Blair JB, Smith D: Quantitative

analysis of glycogen repletion by nuclear magnetic resonance spectroscopy in the conscious rat. *J Clin Invest* 80:387–93, 1987
31. Michal G: *Methods of Enzymatic Analysis*. Vol. 6. Bergmeyer NE, Ed. Weinheim, Germany, VCH, 1985, p. 191–98
32. DeFronzo RA, Diebert D, Hendler R, Felig P, Soman V: Insulin sensitivity and insulin binding to monocytes in maturity-onset diabetes. *J Clin Invest* 63:939–46, 1979
33. Meyer HU, Curchod B, Maeder E, Pahud P, Jequier E, Felber J-P: Modifications of glucose storage and oxidation in nonobese diabetics, measured by continuous indirect calorimetry. *Diabetes* 29:752–56, 1980
34. Boden G, Ray TK, Smith RH, Owen OE: Carbohydrate oxidation and storage in obese non-insulin-dependent diabetic patients: effects of improving glycemic control. *Diabetes* 32:982–87, 1983
35. Yamaguchi A, Chiba T, Yamatani T, Inui T, Morishita T, Nakamura A, Kadowaki S, Masaaki F, Fujita T: Calcitonin gene–related peptide stimulates adenylate cyclase activation via a guanine nucleotide–dependent process in rat liver plasma membranes. *Endocrinology* 123:2591–96, 1988
36. Morishita T, Yamaguchi A, Fujita T, Chiba T: Activation of adenylate cyclase by islet amyloid polypeptide with COOH-terminal amide via calcitonin gene–related peptide receptors on rat liver plasma membranes. *Diabetes* 39:875–77, 1990